High-efficiency resonant amplification of weak magnetic fields for single spin magnetometry at room temperature

High-efficiency resonant amplification of weak magnetic fields for single spin magnetometry at room temperature

Luka Trifunovic,[1] Fabio L. Pedrocchi,[2,1] Silas Hoffman,[1] Patrick Maletinsky,[1] Amir Yacoby,[3,4] and Daniel Loss[1]

[1] *Department of Physics, University of Basel, Klingelbergstrasse 82, CH-4056 Basel, Switzerland*
[2] *JARA Institute for Quantum Information, RWTH Aachen University, D-52056 Aachen, Germany*
[3] *Department of Physics, Harvard University, Cambridge MA, 02138, USA*
[4] *Condensed Matter Chair, Department of Physics and Astronomy, University of Waterloo, Canada*

(Dated: March 2, 2015)

Magnetic resonance techniques not only provide powerful imaging tools that have revolutionized medicine, but they have a wide spectrum of applications in other fields of science like biology, chemistry, neuroscience, and physics. However, current state-of-the-art magnetometers are unable to detect a single nuclear spin unless the tip-to-sample separation is made sufficiently small. Here, we demonstrate theoretically that by placing a ferromagnetic particle between a nitrogen-vacancy (NV) magnetometer and a target spin, the magnetometer sensitivity is improved dramatically. Using materials and techniques already experimentally available, our proposed setup is sensitive enough to detect a single nuclear spin within ten milliseconds of data acquisition at room temperature. The sensitivity is practically unchanged when the ferromagnet surface to the target spin separation is smaller than the ferromagnet lateral dimensions; typically about a tenth of a micron. This scheme further benefits when used for NV ensemble measurements, enhancing sensitivity by an additional three orders of magnitude. Our proposal opens the door for nanoscale nuclear magnetic resonance (NMR) on biological material under ambient conditions.

I. INTRODUCTION

Over the last years, a lot of experimental effort has been put into improving magnetic detection schemes. At present, Hall-sensors and SQUID sensors are among the most sensitive magnetic field detectors.[1,2] Furthermore, a great deal of success has been achieved with magnetic resonance force microscopy, where the force between a magnetic tip and the magnetic moment under investigation is exploited to detect single electron-spins, achieving a resolution of a few cubic nanometers.[3–5] On the other hand, the very low temperatures that are required in such schemes represent a considerable drawback to imaging systems in many biological environments.

NV-center spins also provide very good candidates for magnetometry, boosting sensitivities up to a few $\mathrm{nT}/\sqrt{\mathrm{Hz}}$ at room temperature[6–11] and sub-nanometer spatial resolution, permitting three-dimensional imaging of nanostructures.[7] These results are realizable due to the amazingly long coherence times of NV-centers at room temperature and the ability to noninvasively engineer an NV-magnetometer very close to the magnetic sample. Although impressive, current state-of-the-art technology[12] is unable to detect a single nuclear spin unless the tip-to-sample separation is not made sufficiently small;[13,14] achieving such sensitivity would revolutionize magnetic imaging in chemical and biological systems by facilitating atomic resolution of molecules.

In this work, we propose an experimental realization of NV-magnetometers which do not rely on the cubic dependence of sensitivity on the tip-to-sample separation and are sensitive enough to detect a single nuclear spin within ten milliseconds of data acquisition at room temperature. This can be achieved by introducing a ferromagnetic particle between the spin that needs to be detected, which henceforth we call a qubit,[15] and the NV-magnetometer. When excited on resonance by the driven qubit, the macroscopic ferromagnetic spin begins to precess which, in turn, amplifies the magnetic field felt by the NV-center. By resonantly addressing the qubit and using a ferromagnetic resonator as a lever, our setup, in contrast to existing schemes, is particularly advantageous because, the nuclear spin need not lie within a few nanometers of the surface[16] but rather can be detectable at all distances smaller than the FM lateral dimensions, and, while related existing schemes rely on the *quantum* nature of a mediator spin,[17] our proposal is *fully classical*. With these novelties, our scheme provides chemically sensitive spin detection.

II. SETUP

The standard experimental setup, yielding the most accurate NV-magnetometers (e.g. Ref. 7), consists of an NV-center near the target qubit and two distinct microwave sources that independently control the NV-center and qubit so that double electron-electron (electron-nuclear) resonance, DEER (DENR), can be performed. We extend this setup by including a macrospin ferromagnetic particle (FM) between the NV-magnetometer and the qubit we want to measure, see Fig. 1. A recent experiment[18,19] demonstrates that there is no significant quenching of the NV-center photoluminescence in the presence of the FM. On the other hand, due to the stray field of the FM, the qubit energy-splitting, and therefore the frequency (ω_s) at which the qubit responds resonantly, is strongly modified; one needs first to characterize the FM stray field in order to be able to control the qubit by, in our case, applying π-pulses.[20]

Treating the ferromagnet as a single classical spin, the Hamiltonian of this system is[21,22]

$$H = KV(1 - m_z^2) + M_F V b m_z - \mu_s \boldsymbol{n}_s(t) \cdot \mathbb{B}_F \boldsymbol{m}, \quad (1)$$

where $\boldsymbol{m}$ is the normalized magnetization of the FM, M_F the saturation magnetization of the FM, and V its volume. We assume uniaxial anisotropy in the FM with the anisotropy constant, $K > 0$, composed of both shape and crystalline anisotropy, with an easy axis along z. An external magnetic field b is applied along the z axis. The magnetic moment of the qubit is μ_s and $\boldsymbol{n}_s(t)$ is its polarization at time t. The 3×3-matrix $\mathbb{B}_F$ is defined as $(\mathbb{B}_F)_{ij} = \boldsymbol{B}_F^j(\boldsymbol{r}_s) \cdot \boldsymbol{e}_i$, where $\boldsymbol{B}_F^j(\boldsymbol{r}_s)$ is the stray field produced by the FM at the position of the qubit, $\boldsymbol{r}_s$, when the FM is polarized along the j-axis for $j = x$, y, or z. The Hamiltonian of the qubit is not explicitly written as its polarization is completely determined by the externally applied static and time-dependent microwave field and the stray field of the FM. For example, in equilibrium the ground state of the qubit is polarized along the total static field acting on it $\boldsymbol{n}_s = (\boldsymbol{b} \pm \boldsymbol{B}_F^z)/|\boldsymbol{b} \pm \boldsymbol{B}_F^z|$ when $m_z = \pm 1$. Although in the following we take V small enough to approximate the FM as a monodomain, our analysis and therefore our results are amenable to including the effects of magnetic texture.

Using two independent microwave sources we apply a train of π-pulses first to the qubit and subsequently a Carr-Purcell-Meiboom-Gill (CPMG) pulse sequence[23,24] to the NV-center, see Fig. 2. As the qubit is pulsed it will drive the FM at the frequency of the pulse sequence π/τ, τ being the time between the application of two subsequent π-pulses. When π/τ is close to the ferromagnetic resonance (FMR) frequency, ω_F, the response of the FM becomes large and one obtains a large amplification of the magnetic field felt by the NV-center. The pulses are applied to the qubit only until the FM reaches steady state precession. We also allow for a possible time offset, ξ, between the pulse sequences applied to the qubit and the NV-center, see Fig. 2. Here, ξ may be chosen to compensate for the phase difference between the driving of the qubit and the response of the FM, thus maximizing the sensitivity of our magnetometry scheme. Since the microwave field applied to the qubit is a sequence of π-pulses, the polarization is simply $\boldsymbol{n}_s(t) = \boldsymbol{n}_s f_\tau(t)$, where $f_\tau(t)$ may take the values ± 1 according to the pulse sequence. It is worth noting that even though we excite the FMR with the inhomogeneous dipolar field of the qubit, only the lowest Kittel mode is excited since for a small FM higher modes are separated by an energy gap that exceeds the perturbation amplitude. Therefore the macrospin approximation used in Eq. (1) is justified.

III. PROPOSED MAGNETOMETER SENSITIVITY

We now consider our particular scenario wherein a FM is introduced at a distance d from the qubit and h from the NV-center (Fig. 1). In this case, both the accumulated phase and the dephasing of the NV-center are modified by the presence of the FM. Because the sensitivity of our magnetometry scheme crucially depends on the series of pulses applied to the NV-center and qubit, here we detail the pulse sequence, see Fig. 2. First we apply, on the qubit only, N' π-pulses separated by a time interval τ, for a total time of $t' = N'\tau$—during this time the FM reaches steady state precession. Next we initialize the NV-center in state $|0\rangle$, which takes time t_p that is on the order of few hundreds of nanoseconds. Then, a $\pi/2$ pulse is applied to the NV-center allowing it to accumulate the

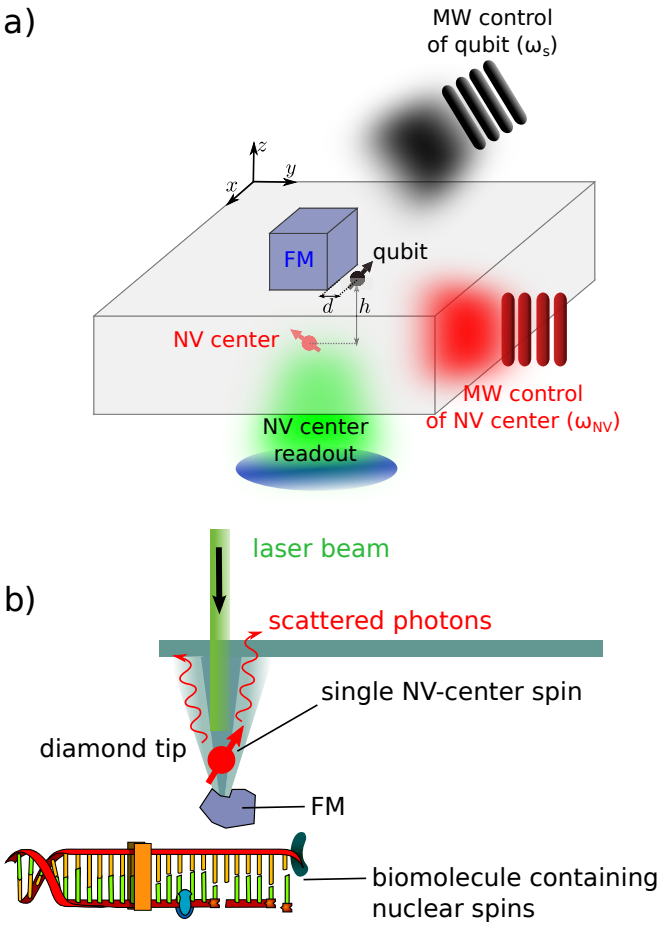

Figure 1. Panel a) shows a detailed illustration of the setup considered. The abbreviation "FM" denotes the ferromagnetic particle that is placed on top of the diamond surface that contains the NV-center (red) which is used as magnetometer. Close to the top surface of the FM lies the qubit (black) we want to measure. The setup also includes separate microwave (MW) controls of the qubit (black) and NV-center (red) with resonance frequencies ω_s and $\omega_{\rm NV}$, respectively. The ferromagnetic resonance frequency ω_F is assumed to be different from both ω_s and $\omega_{\rm NV}$. The NV-center is read out optically with a green laser. A slightly modified version of the setup with the NV-center and the FM on a tip is illustrated in panel b); for simplicity we have omitted the two driving fields in this panel.

phase from the FM tilt stray field. Consequently, a series of N π-pulses are applied to both the NV-center and qubit for a total interrogation time $t_i = N\tau$. Finally we apply to the NV-center a $\pi/2$-pulse which is, in general, along an axis in the plane orthogonal to the NV-center axis and different from the first $\pi/2$-pulse by an angle θ. The probability that the NV-center occupies the state $|0\rangle$ or $|1\rangle$ after the pulse sequence is now a function of the accumulated phase $\varphi_{\rm NV}(t_i)$

$$p(n|\varphi_{\rm NV}(t_i)) = \frac{1}{2}\left(1 + n\cos(\varphi_{\rm NV}(t_i) + \theta)e^{-\langle(\delta\varphi_{\rm NV}(t_i))^2\rangle}\right). \tag{2}$$

Here, $n = \pm 1$ are the two possible outcomes when the state of the NV-center is measured, $\langle(\delta\varphi_{\rm NV}(t_i))^2\rangle$ is the dephasing of the NV-center, and $\langle\cdots\rangle$ is the expectation value in the Gibbs state. Because the accumulated phase itself depends on the value of the qubit magnetic moment μ_s, a measurement of the NV-center is a measurement of μ_s. The variance in the measured value of the NV-center can be reduced by repeating the measurement $\mathcal{N}$ times (Fig. 2). Because typically $t' \ll \mathcal{N}t_i$ and therefore $t' + \mathcal{N}t_i \approx \mathcal{N}t_i$, the total measurement time is marginally prolonged by the initial pulse sequence that initialized the tilt of the FM.

Given Eq. (2), one may show quite generally that the sensitivity of the NV-magnetometer is given by

$$S = \frac{1}{R\sqrt{\eta}}\min_{t_i}\left[\frac{e^{\langle(\delta\varphi_{\rm NV}(t_i))^2\rangle}\sqrt{t_i + t_p}}{|\partial\varphi_{\rm NV}(t_i)/\partial\mu_s|}\right], \tag{3}$$

which defines the minimum detectable magnetic field for a given total measurement time. Here, R, the measurement contrast, is the relative difference in detected signal depending on spin-projection of the NV-center spin, and η is the detection efficiency which takes into account that many measurements have to be performed in order to detect a photon.[25] A detailed derivation of Eq. (3) can be found in Supplementary Information, Sec. II. The sensitivity is small (*i.e.*, 'good') when the NV-center dephasing is small while the accumulated phase is large. When the qubit is directly coupled to the NV-center (without the FM) the dephasing time of the NV-center is given by $T_2 \sim 200$ μs[26,27] so that $\langle(\delta\varphi_{\rm NV}(t_i))^2\rangle = (t_i/T_2)^2$.

As we show in Supplementary Information, Sec. IV, given the pulse sequence described above, when $\Gamma t' \gg 1$ and $\Gamma t_i \ll 1$, where Γ is the linewidth of the ferromagnet, there is a *resonant* response of the FM while the NV-center picks up *non-resonant* noise. As such, the ratio of the dephasing to the accumulated phase of the qubit is minimized thereby optimizing the sensitivity. We henceforth take $\Gamma t' \gg 1 \gg \Gamma t_i$ in the remainder of the text.

The accumulated phase is formally

$$\varphi_{\rm NV}(t_i) = \gamma_{\rm NV}\int_0^{t_i} B_{\rm NV}(t'')f_\tau(t'')dt'', \tag{4}$$

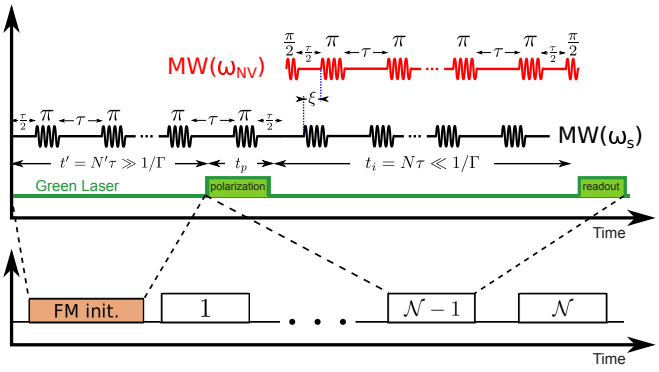

Figure 2. The pulse sequence that we apply to the qubit (black) and to the NV-center spin (red). The pulse sequence $f_\tau(t)$ that consists of N (N is even) is applied to both spins, with the time offset ξ, during the interrogation time $t_i = N\tau$. The measurement is repeated $\mathcal{N}$ times until the desired precision is achieved, as illustrated on the bottom panel. The sequence section denoted by "FM init" with duration $t' = N'\tau$ is the time during which the precession of the FM is being developed. We assume that the frequencies ω_s, $\omega_{\rm NV}$, and ω_F are all sufficiently different from each other. The green laser is applied to the NV-center for initialization (polarization) and read-out. The total measurement time is $t' + \mathcal{N}t_i \approx \mathcal{N}t_i$.

where $\gamma_{\rm NV}$ is the gyromagnetic ratio of the NV. $B_{\rm NV} \equiv \left|\boldsymbol{B}^-_{F,\rm NV}\cdot\boldsymbol{n}_{\rm NV}\right|$ where $\boldsymbol{B}^\pm_{F,\rm NV} = \boldsymbol{B}^x_F(\boldsymbol{r}_{\rm NV}) \pm i\boldsymbol{B}^y_F(\boldsymbol{r}_{\rm NV})$ [$\boldsymbol{B}^\pm_{F,s} = \boldsymbol{B}^x_F(\boldsymbol{r}_s) \pm i\boldsymbol{B}^y_F(\boldsymbol{r}_s)$] is a complex combination of the magnetic stray-field for the FM polarization along the x and y axes at the position of the NV-center (qubit), $\boldsymbol{r}_{NV}$ ($\boldsymbol{r}_s$), and $\boldsymbol{n}_{\rm NV}$ is the NV-center polarization axis. We note that $\boldsymbol{B}^\pm_{F,\rm NV}\cdot\boldsymbol{n}_{\rm NV}$ ($\boldsymbol{B}^\pm_{F,s}\cdot\boldsymbol{n}_s$) is the FM-NV (FM-qubit) coupling constant.

Within the linear response regime and using the pulse sequence described above and optimally choosing ξ, the expression for the phase accumulated by the NV-center when $\tau = (2k+1)\pi/\omega_F$,[28] for $k = 0, 1, \ldots$, is

$$\varphi_{\rm NV}(t_i) = \frac{4\mu_s\gamma\gamma_{\rm NV}|\boldsymbol{B}^+_{F,s}\cdot\boldsymbol{n}_s||\boldsymbol{B}^-_{F,\rm NV}\cdot\boldsymbol{n}_{\rm NV}|}{\pi^2(2k+1)^2M_FV\Gamma}t_i, \tag{5}$$

where γ is the gyromagnetic ratio of the FM. k is defined such that the resonantly driven FM undergoes $2k+1$ half-periods between consecutive π-pulses applied to the NV-center. In the optimal case we have $k = 0$ so that τ is half the period of precession of the ferromagnet. The details of the derivation of Eq. 5 can by found in Supplementary Information, Sec. IV. It is readily observed from the above equation that $\varphi_{\rm NV}(t_i) \sim 1/\Gamma$ which is proportional to the AC magnetic susceptibility of the FM on resonance; thus we indeed obtain a resonant response as anticipated. Even though the phase $\varphi_{\rm NV}$ accumulated due to the FM tilt is large, the angle of the FM tilt is small ($\sim 10^{-3}$ if the qubit is a nuclear spin) because $M_FV \gg \mu_s$. Therefore, we can neglect the effects of the backaction of the FM tilt on the qubit, because the stray field modulation induced by the tilt is

small compared to the qubit Rabi amplitude and far detuned from the qubit Larmor precession frequency (i.e. $\omega_F \neq \omega_s$). Thus, the qubit is polarized along the total field $\boldsymbol{n}_s = (\boldsymbol{B}_F^z + \boldsymbol{b})/|\boldsymbol{B}_F^z + \boldsymbol{b}|$; the scalar product $\boldsymbol{B}_{F,s}^+ \cdot \boldsymbol{n}_s$ is nonzero only if the stray field of the FM tilt has a component along $\boldsymbol{n}_s$ at the position of the qubit. We address the optimal geometry and position of the qubit relative to the FM in Methods, Sec. VI B.

The relevant dephasing is the maximum of the inherent dephasing of the NV-center, $(t_i/T_2)^2$, and the dephasing due to the coupling to the FM,[23]

$$\beta(t_i,\tau) = \gamma_{\rm NV}^2 \int_0^{t_i} ds S(s) \int_0^{t_i - s} dt'' f_\tau(t'') f_\tau(t''+s). \quad (6)$$

Here $S(s) = \langle B_{\rm NV}(s) B_{\rm NV}(0)\rangle$ is the autocorrelation function of the FM noise. Again taking $\tau = (2k+1)\pi/\omega_F$, we show in Supplementary Information, Sec. IV B that

$$\beta(t_i,\tau) = \frac{4\gamma\gamma_{\rm NV}^2 |\boldsymbol{B}_{F,\rm NV}^+ \cdot \boldsymbol{n}_{\rm NV}|^2 k_B T}{\pi^2 (2k+1)^2 M_F V \omega_F} t_i^2 \equiv (t_i/T_2')^2 , \quad (7)$$

where T_2' (T_2) is the decoherence time of the NV-center caused by the FM. Because $\beta(t_i,\tau) \sim 1/\omega_F \sim S(\omega = 0)$, the NV-center indeed accumulates non-resonant noise.

The value of the NV-center decoherence rate when the FM volume is chosen as small as possible (see Eq. 9) becomes $T_2'^{-1} \sim \gamma_{\rm NV} |\boldsymbol{B}_{F,\rm NV}^+ \cdot \boldsymbol{n}_{\rm NV}|$. Furthermore, since the optimal interrogation time is $t_i \sim T_2'$, we obtain that for typical values of the FM stray field we are in the limit $t_i \ll t_p$. After substituting $\langle (\delta\varphi_{\rm NV}(t_i))^2\rangle = \beta(t_i,\tau)$ and $\varphi_{\rm NV}(t_i)$ from Eq. (5) and Eq. (7) into Eq. (3) and performing the minimization over the interrogation time in Eq. (3), we find the sensitivity S_A of our magnetometry scheme

$$S_A = \frac{1}{R\sqrt{\eta}} \frac{\pi e^{\frac{1}{2}} (2k+1) M_F V \Gamma}{\sqrt{2}\gamma |\boldsymbol{B}_{F,s}^+ \cdot \boldsymbol{n}_s|} \sqrt{\frac{\gamma k_B T t_p}{M_F V \omega_F}}. \quad (8)$$

The best sensitivity is obtained when one half-period of the FM oscillation occurs over the timescale τ, *i.e.*, $k = 0$. In practice, experimental limitations, such as limitations to the qubit Rabi frequency, bound τ and therefore k from below. Thus, in order to achieve the resonance, one has to use $k \gg 0$ (at the expense of sensitivity) or to tune the FMR frequency as described in the following subsection. We note that since the sensitivity in Eq. 8 scales as $S_A \sim \Gamma$, using low loss FM materials like Yttrium Iron Garnet (YIG) is crucial for achieving high sensitivities.

A few comments are in order regarding the obtained expression for the sensitivity in Eq. 8. First, we note that S_A is completely independent of the FM-NV coupling constant $|\boldsymbol{B}_{F,\rm NV}^{\pm} \cdot \boldsymbol{n}_{\rm NV}|$—this behavior holds as long as the stray field at position of the NV is not too weak, since otherwise a weak FM-NV coupling leads to long T_2' and thus we are no longer in the limit $t_i \ll t_p$ and thus Eq. 8 is no longer valid. Therefore, S_A depends only on d but not on h (see Fig. 1). Having a magnetometer with the sensitivity that is independent of the NV positioning[29] is particularly advantageous for NV ensemble measurements since we can place many NV-centers that would all have the same sensitivity (though different optimal interrogation times) and thus obtain significant improvement of the total sensitivity. Finally, S_A depends on the FM-qubit coupling constant and therefore depends on d. But herein, rather than having a sensitivity that has cubic dependence on the tip-to-sample separation, we have only weak dependence on d since the FM stray field is not changed much as long as $d \ll L \equiv V^{1/3}$ (see Methods, Sec. VI B). The spatial resolution of our scheme does not differ from the standard NV-magnetometry resolution.[7] In practice the spatial resolution for detection of an isolated spin is determined by the ratio between the magnetic field gradient and the target qubit linewidth. In the case of interacting spins there is a broadening caused by homonuclear dipolar interaction, thus the techniques such as magic angle spinning (MAS) should be used.[30] Since MAS is usually performed by spinning the sample in a static magnetic field which is impractical for our scheme, one can use rotating magnetic fields[31] instead, with the frequency different from ω_{NV}, ω_F and ω_s for performing MAS.

While the electron spin in a NV-center can be driven at GHz frequencies,[32,33] the same driving field for a proton spin would yield Rabi frequency in the MHz range. Thus, the FMR frequency needs to be tuned to meet the resonance critieria. The method to achieve such a tuning is described in Methods, Sec. VI A. The idea is to use the metastable state of the FM which has frequency that can be lowered by applying an external magnetic field. In order for the FM to remain in the metastable state during the measurement time, the FM volume must satisfy

$$V \gtrsim \frac{\gamma k_B T}{M_F \omega_F^+} |\ln \alpha|, \quad (9)$$

In case of minimal volume, the sensitivity reads

$$S_A = \frac{1}{R\sqrt{\eta}} \frac{\pi (2k+1) \alpha \sqrt{e |\ln\alpha| t_p} k_B T}{\sqrt{2} |\boldsymbol{B}_{F,s}^+ \cdot \boldsymbol{n}_s|} . \quad (10)$$

As noted earlier, the sensitivity of our scheme does not depend on the FM-NV coupling constant. Thus, we can take advantage of this fact to obtain an improvement of sensitivity by a factor of $\sqrt{N_{\rm NV}}$, when $N_{\rm NV}$ NV-centers are used for the detection. We present a detailed discussion in Sec. VI C of the Methods.

A. Estimates

In this section we give estimates for the sensitivity S_A for two cases: with and without tuning of the FMR frequency (to MHz range). We also provide the estimates for the case when an NV ensemble is used for the measurement. For all the estimates provided in the following, we assume room temperature and that the FM material is YIG, so that $\alpha \sim 10^{-5}$, $\mu_0 M_F = 0.185$ T, and

$K/M_F = 60$ mT.[34] For simplicity but without loss of generality, we assume that the FM has the shape of a cube for the estimates given below. For a cube and in the macrospin approximation there is no contribution from shape anisotropy.

If we tune the FMR frequency to MHz range the minimum FM volume V according to Eq. (9) corresponds to a cube with side $L = 210$ nm. We note that since $t_i \ll t_p \ll \tau$ (see Fig. 2) one essentially performs DC magnetometry with the NV. Furthermore, S_A being weakly dependent on d for $d \ll L$ means that we can increase the "FM surface"-to-"target spin" separation up to values of hundred nanometers practically without decreasing the sensitivity S_A. Taking $t_p \sim 300$ ns and estimating $R\sqrt{\eta}$ from Ref. 6, we obtain $S_A = 0.13\mu_N/\sqrt{\text{Hz}}$, where μ_N is the nuclear magneton. Thus, our magnetometry scheme can detect a single nuclear spin within ten milliseconds of data acquisition at room temperature. For comparison, standard NV-magnetometry setups with the state-of-the-art magnetic field sensitivity[35] $S = 4.3$ nT$/\sqrt{\text{Hz}}$ needs a ∼100 times smaller tip-to-sample separation[13,14] of 2.5 nm in order to achieve the same magnetic moment sensitivity.

For the electron spin, the minimal FM volume V according to Eq. (9) corresponds to a cube with side $L = 21$ nm in this case. Using the same parameters as in the previous paragraph we obtain $S_A = 0.32\mu_N/\sqrt{\text{Hz}}$.

Typical values of the stray fields at the position of the qubit and NV-center in the limit $d, h \ll L$ for YIG are on the order of a few hundreds of Gauss. The presence of a magnetic field perpendicular to the NV-center axis can significantly limit the read-out fidelity of the NV-center, it was found that fields up to 100 Gauss can be tolerated.[36] Since the sensitivity S_A does not depend on the FM-NV coupling constant, the NV should be placed in the region where the stray field $B_{F,\text{NV}}$ is less than 100 Gauss but bigger than the threshold value B_{th}, i.e., 1 Gauss $< B_{F,\text{NV}} <$ 100 Gauss. For $|\boldsymbol{B}^{\pm}_{F,\text{NV}} \cdot \boldsymbol{n}_{\text{NV}}| \sim 10$ Gauss, the decoherence time of the NV is $T_2' \sim 100$ ns [see Eq. (7)], which is also the value of the optimal interrogation time. Thus, because the signal amplification in our scheme far exceeds the effect of the additional decoherence it induces, even shallow NV-centers[26,27] or dense ensembles of NV-centers[25] with relatively short decoherence time can be used and significantly outperform long-lived NV-centers (without the FM).

Finally, we give the estimates for the case of the FMR tuned to the MHz range and for measurements with ensembles of NV-centers. As experimentally demonstrated,[37] NV ensembles with a separation of about 10 nm between neighboring NV-centers can be achieved. Such NV ensembles have $T_2^* \sim 100$ ns, but this property, as noted in the previous paragraph, does not affect the sensitivity of our scheme. We can distribute the NV-centers in the volume where the stray field satisfies $B_{F,\text{NV}} > B_{\text{th}}$ and such a volume can be estimated to be a cube with side length of 1 μm. Therefore, $N_{\text{NV}} \sim 10^6$ which yields an unprecedented sensitivity of $\tilde{S}_A = 0.13 \times 10^{-3}\mu_N/\sqrt{\text{Hz}}$.

IV. CONCLUSIONS

We have proposed and analyzed, both analytically and numerically, a modification of a standard NV-magnetometry setup that yields a significant improvement of NV-magnetometer sensitivity—the obtained sensitivity is practically unchanged as long as the ferromagnet surface to the target spin separation is smaller than the ferromagnet lateral dimensions which is typically about a tenth of a micron. Our scheme is based on a ferromagnetic particle, placed in close proximity to a sensing NV-center spin. The qubit spin to be detected is then used to resonantly drive the large macrospin of the FM giving rise to a strong, amplified stray field acting on the NV-magnetometer. Compared to the existing schemes that use the quantum nature of an intermediate spin for improving sensitivity,[17] we stress that our scheme is fully classical and thus should be easily realizable at room temperature—all the ingredients of our scheme are already demonstrated in separate experiments.[7,18,19,32,33,38,39]

The magnetometric scheme including a ferromagnetic particle proposed here is a step forward to a more accurate magnetic field measurement. In particular, it enables the detection of a single nuclear spin at distances that are noninvasive to the system under study. Therefore, the proposed room temperature magnetometry scheme opens up new venues for future analyses of previously inaccessible biological and chemical systems.

V. ACKNOWLEDGMENTS

We would like to thank H. Fanghor for sharing his expertise about micromagnetic simulations. This work was supported by the SNF, NCCR QSIT, IARPA, DARPA QuASAR programs and the MURI QuISM. F. L. P. is grateful for support from the Alexander von Humboldt foundation.

VI. METHODS

A. Tuning the FMR frequency

It has been demonstrated experimentally[32,33] that the electron spin of NV-centers can be coherently driven at GHz frequency. For a proton spin, however, the same drive would yield Rabi oscillations in the MHz range. Because typical FMR frequencies are in GHz range, ω_F needs to be reduced in order for the proton Rabi frequency to be on resonance with the FMR.

One way to decrease ω_F is to apply an external magnetic field antiparallel to $\boldsymbol{m}$,[40] whereby there is a

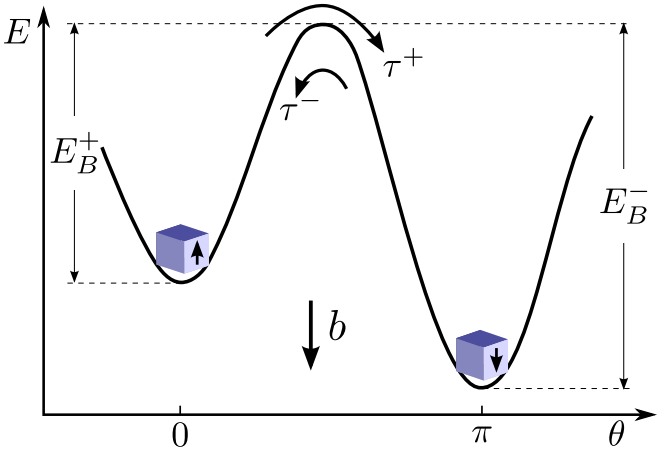

Figure 3. The FM energy when an external field $b/b_a = 0.2$ is applied, *i.e.*, the first two terms from the right-hand side of Eq. (1) of the main text, as a function of θ, where $m_z = \cos\theta$. The metastable state at $\theta = 0$ has smaller FMR frequency compared to the case with no external field. The tunneling time τ^+ from the metastable state has to be longer than the measurement time. We note that $E_B^+ = M_F V(b_a - b)$.

metastable state when $b < b_a$, with $b_a = K/M_F$ the FM (crystalline and shape) anisotropy field. In Fig. 3, we plot the energy of the FM as a function of angle θ of the magnetization with respect to the easy axis, according to Eq. (1) of the main text. It is straightforward to show that the FMR frequency in the metastable state is $\omega_F^+ = \gamma(b_a - b)$. On the other hand, the ferromagnet will relax to the thermal state on a timescale τ^+ given by the Arrhenius law $\tau^+ = \tau_0 e^{E_B^+/k_B T}$, where $\tau_0 \sim 1/\omega_F^+$ is the attempt time. We can insure that the FM is initialized in the metastable state by first measuring the direction of the magnetization, applying an external magnetic field $\boldsymbol{b}$ antiparallel to $\boldsymbol{m}$ and checking subsequently that the FM magnetization direction is unchanged, which can be done under hundred picoseconds.[41–43] In order for the ferromagnet to remain in the metastable state while the measurement is being performed, we require $\tau^+ \gg 1/\Gamma$. Indeed, the total measurement time T should be larger than the FMR initialization time $t' \gg 1/\Gamma$, and smaller than Arrhenius' timescale $\tau^+ \gtrsim T$, see Fig. 2 in the main text. Thus, if we want to tune ω_F^+ to a certain value and work at room temperature, the Arrhenius law suggests that the FM volume must satisfy

$$V \gtrsim \frac{\gamma k_B T}{M_F \omega_F^+} |\ln \alpha|, \tag{11}$$

in order for the metastable state lifetime to be bigger than the measurement time. Here $\alpha = \Gamma/\omega_F^+$ is the Gilbert damping of the FM. Substituting Eq. (9) for the minimal volume into Eq. (8) of the main text we obtain

$$S_A = \frac{1}{R\sqrt{\eta}} \frac{\pi(2k+1)\alpha\sqrt{e|\ln\alpha| t_p} k_B T}{\sqrt{2}|\boldsymbol{B}_{F,s}^+ \cdot \boldsymbol{n}_s|} \tag{12}$$

Compared to the sensitivity in Eq. (8) of the main text, the above expression is independent of the FMR frequency ω_F and the FM volume V. Thus, irrespective of the choice of the frequency we work at, the same value for the sensitivity S_A is obtained. Furthermore, the only dependence on the volume is incorporated in the stray fields but, as shown in Sec. VI B, this dependence is weak in the limit $d \ll L$. The volume in Eq. (9) is implicitly bounded from above in order to remain in the regime where the macrospin approximation is valid.

An alternative setup to achieve resonance between the qubit and FM is to place the NV-center and the FM on a cantilever[44] with resonance frequency in the GHz range. By driving the cantilever, we alleviate the necessity of driving the qubit at FMR frequency as the qubit field is modulated by the oscillations of the cantilever. Since the dipolar field of the qubit decays rapidly with distance, the modulation of the qubit field achieved in this scheme is almost as big as when the qubit is driven via a microwave field (the previously described scheme for which the sensitivity estimates are given). Therefore, we conclude that the estimates for the sensitivity S_A given in Sec. III A still hold in that case.

B. FM geometry and demagnetizing fields

In the absence of an external magnetic field, the qubit aligns along the stray field direction of the FM, while the FM spins are aligned along the easy axis. Because $M_F V \gg \mu_s$, the FM tilt induced by the qubit is negligible. Therefore, the qubit will align along the direction of the stray field produced by the FM. However, for most geometries of the FM and positions of the qubit, the FM-qubit coupling constant is almost zero, i.e. $|\boldsymbol{B}_{F,s}^+ \cdot \boldsymbol{n}_s| \sim \boldsymbol{B}_{F,s}^{x,y} \cdot \boldsymbol{B}_{F,s}^z \sim 0$, and therefore the sensitivity is bad $S_A^{-1} \sim 0$. In the following discussion, we consider our ferromagnet to be a cube of side L, but our conclusions can be straightforwardly generalized to other geometries. To gain insight into the direction and strength of the stray field, we use the well-known analogy between the stray field of a homogeneously magnetized body and an electric field produced by surface charges. Specifically, we may consider the surfaces of the cube to have charge density $\sim M_F\, \boldsymbol{m} \cdot \boldsymbol{s}$, where $\boldsymbol{s}$ is the vector normal to the surface of the cube. Therefore, when the position of the qubit is very close to the center of the FM surface which is perpendicular to the polarization direction (here assumed along z-axis), $\boldsymbol{B}_{F,s}^z$ points along the z-axis. Similarly, $\boldsymbol{B}_{F,s}^x$ and $\boldsymbol{B}_{F,s}^y$ are almost aligned with the x and y axes close to the surface, respectively. Therefore, in these positions, $\boldsymbol{B}_{F,s}^{x,y} \cdot \boldsymbol{B}_{F,s}^z \sim 0$. However, this is not true near the edges of the ferromagnet. Therefore, in order to obtain a sensitive magnetometer, one needs, first, a ferromagnet with edges and, second, to position the qubit close to the edges. One may show analytically and numerically (see Fig. 4) that $|\boldsymbol{B}^+ \cdot \boldsymbol{n}_s|/|B^+|$ close to the edges is about an order of magnitude bigger than close to the face

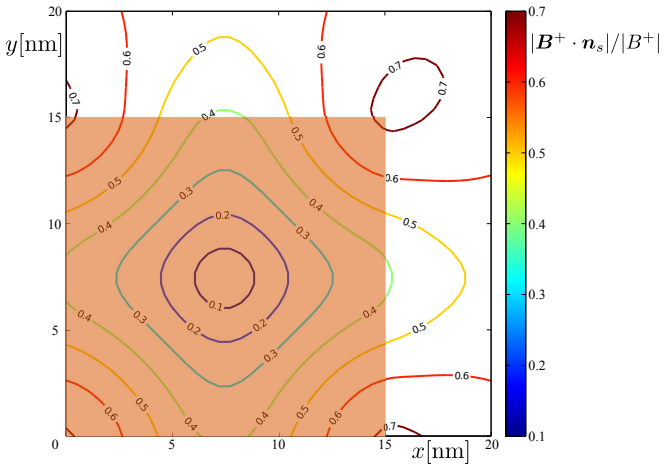

Figure 4. Contour plot of the quantity $|\boldsymbol{B}^+ \cdot \boldsymbol{n}_s|/|B^+|$ in the xy-plane that is 2 nm above the upper face of the cube. We assume the FM cube (orange square) has a side length of $L = 15$ nm. The values of the stray fields are obtained from OOMMF micromagnetic simulations, taking into account the demagnetizing field.

center and that it has local maxima close to the cube's corners. In evaluating $\boldsymbol{B}_{F,s}^{x,y,z}$, we assume that the FM is homogeneously magnetized as, in cubic geometry, one can find an analytical formula for the stray field in this case (see Supplementary Information, Sec. V). However, it is important to note that due to demagnetizing fields (arising from dipole-dipole interactions in the FM), the FM ground-state is not homogeneous but rather "flower-like".[45] Specifically, the canting of the spins close to the edges is more pronounced,[46] which modifies the FM stray field close to the edges. To account for the effects of the demagnetizing fields, we perform micromagnetic simulations in OOMMF.[47] In Fig. 4 we plot $|\boldsymbol{B}^+ \cdot \boldsymbol{n}_s|/|B^+|$ in the xy-plane that is 2 nm above the upper face of the cube. We find that the inclusion of demagnetizing fields changes our value of $\boldsymbol{B}_{F,s}^{x,y,z}$ by only $\sim 1\%$ as compared to the uniformly magnetized cube. Therefore, we expect the analytical expression for the stray field to be valid for our choice of parameters.

Because the sensitivity S_A depends on d only through the stray field at the position of the qubit, herein we detail this dependence and show that the sensitivity of our magnetometry scheme is practically unchanged as d is varied. The stray field close to the cube edge (in comparison to L) is equivalent to the electric field of a set of infinite line charges. Therefore, there is a logarithmic dependence of the stray field on the distance to the edge, d, of the cube in units of L so that the sensitivity S_A is only weakly dependent on d.

C. NV ensemble measurements

As noted earlier, the sensitivity of our scheme S_A does not depend on the FM-NV coupling constant. Such behavior of the sensitivity is in stark contrast to the cubic dependence on the tip-to-sample separation of typical NV-magnetometer sensitivity. This property of S_A is very useful if we want to perform the measurements with an ensemble of NV-centers since all of them would have the same sensitivity irrespective of the actual value of the FM-NV coupling constant. Thus, we obtain an improvement of sensitivity by a factor of $\sqrt{N_{\rm NV}}$, where $N_{\rm NV}$ is the number of NV-centers in the ensemble. In our scheme $N_{\rm NV}$ is the maximum number of NV-centers that we can place in the region of space around the FM where the stray field value is above the threshold $B_{\rm th}$.

As the FM volume is increased, the sensitivity is decreased as $S_A \sim \sqrt{V}$ see Eq. 8. Nevertheless, in case of an NV ensemble measurement, increasing V leads to an increase of $N_{\rm NV}$ V. Thus, for ensemble measurements our scheme does not loose sensitivity when the FM volume is increased, but rather the sensitivity is logarithmically improved due to increasing the FM-qubit coupling constant. The possibility of having a large FM without loss of sensitivity is important since it can be experimentally more feasible to work with micron-sized FMs.

[1] E. Ramsden, *Hall-Effect Sensors, Second Edition: Theory and Application*, 2nd ed. (Newnes, Amsterdam ; Boston, 2006).
[2] M. E. Huber, N. C. Koshnick, H. Bluhm, L. J. Archuleta, T. Azua, P. G. BjÃ¶rnsson, B. W. Gardner, S. T. Halloran, E. A. Lucero, and K. A. Moler, Rev. Sci. Instrum. **79** (2008).
[3] C. L. Degen, M. Poggio, H. J. Mamin, C. T. Rettner, and D. Rugar, Proc. Natl Acad. Sci. USA **106**, 1313 (2009).
[4] M. Poggio and C. L. Degen, Nanotechnology **21**, 342001 (2010).
[5] P. Peddibhotla, F. Xue, H. I. T. Hauge, S. Assali, E. P. A. M. Bakkers, and M. Poggio, Nat Phys **9**, 631 (2013).
[6] H. J. Mamin, M. Kim, M. H. Sherwood, C. T. Rettner, K. Ohno, D. D. Awschalom, and D. Rugar, Science **339**, 557 (2013).
[7] M. S. Grinolds, M. Warner, K. D. Greve, Y. Dovzhenko, L. Thiel, R. L. Walsworth, S. Hong, P. Maletinsky, and A. Yacoby, Nat. Nano. **9**, 279 (2014).
[8] T. Staudacher, F. Shi, S. Pezzagna, J. Meijer, J. Du, C. A. Meriles, F. Reinhard, and J. Wrachtrup, Science **339**, 561 (2013).
[9] L. Rondin, J. P. Tetienne, T. Hingant, J. F. Roch, P. Maletinsky, and V. Jacques, Rep. Prog. Phys. **77**, 056503 (2014).
[10] G. Waldherr, J. Beck, P. Neumann, R. S. Said, M. Nitsche, M. L. Markham, D. J. Twitchen, J. Twamley, F. Jelezko, and J. Wrachtrup, Nat Nano **7**, 105 (2012).
[11] L. C. Bassett, F. J. Heremans, D. J. Christle, C. G. Yale, G. Burkard, B. B. Buckley, and D. D. Awschalom, Science

(2014).
[12] P. Maletinsky, S. Hong, M. S. Grinolds, B. Hausmann, M. D. Lukin, R. L. Walsworth, M. Loncar, and A. Yacoby, Nat. Nano **7**, 320 (2012).
[13] M. Loretz, T. Rosskopf, J. M. Boss, S. Pezzagna, J. Meijer, and C. L. Degen, Science (2014), 10.1126/science.1259464.
[14] A. O. Sushkov, I. Lovchinsky, N. Chisholm, R. L. Walsworth, H. Park, and M. D. Lukin, Phys. Rev. Lett. **113**, 197601 (2014).
[15] We emphasize that we denote the target magnetic moment by 'qubit' solely for the purpose of convenience in nomenclature and that our scheme does not rely on the quantum nature of the magnetic moment we aim to measure.
[16] M. Loretz, S. Pezzagna, J. Meijer, and C. L. Degen, App. Phys. Lett. **104** (2014).
[17] M. Schaffry, E. M. Gauger, J. J. L. Morton, and S. C. Benjamin, Phys. Rev. Lett. **107**, 207210 (2011).
[18] T. van der Sar, F. Casola, R. Walsworth, and A. Yacoby, arXiv:1410.6423 (2014).
[19] C. S. Wolfe, V. P. Bhallamudi, H. L. Wang, C. H. Du, S. Manuilov, R. M. Teeling-Smith, A. J. Berger, R. Adur, F. Y. Yang, and P. C. Hammel, Phys. Rev. B **89**, 180406 (2014).
[20] Instead of performing the qubit control resonantly, one can make use of 'adiabatic passage'[48] wherein triangular pulses are applied in lieu of square pulses. In such a setup, knowledge of the exact value of the qubit Zeeman splitting, and therefore the FM stray field, is not needed.
[21] E. C. Stoner and E. P. Wohlfarth, Phil. Trans. R. Soc. A **240**, 599 (1948).
[22] L. Trifunovic, F. L. Pedrocchi, and D. Loss, Phys. Rev. X **3**, 041023 (2013).
[23] Å. CywiÅski, R. M. Lutchyn, C. P. Nave, and S. Das Sarma, Phys. Rev. B **77**, 174509 (2008).
[24] G. de Lange, Z. H. Wang, D. RistÃ, V. V. Dobrovitski, and R. Hanson, Science **330**, 60 (2010).
[25] V. M. Acosta, E. Bauch, M. P. Ledbetter, C. Santori, K.-M. C. Fu, P. E. Barclay, R. G. Beausoleil, H. Linget, J. F. Roch, F. Treussart, S. Chemerisov, W. Gawlik, and D. Budker, Phys. Rev. B **80**, 115202 (2009).
[26] K. Ohno, F. Joseph Heremans, L. C. Bassett, B. A. Myers, D. M. Toyli, A. C. Bleszynski Jayich, C. J. Palmstrom, and D. D. Awschalom, App. Phys. Lett. **101**, 082413 (2012).
[27] B. A. Myers, A. Das, M. C. Dartiailh, K. Ohno, D. Awschalom, D., and C. Bleszynski Jayich, A., Phys. Rev. Lett. **113**, 027602 (2014).
[28] The Fourier transform of the CPMG pulse sequence has peaks at frequencies $(2k+1)\pi/\tau$.
[29] We stress that this statement is true only in region of space near the FM where $T_2' \ll t_p$, i.e., where the FM stray field is bigger that the threshold value $B_{\rm th} \sim 1$ Gauss.
[30] G. Puentes, G. Waldherr, P. Neumann, G. Balasubramanian, and J. Wrachtrup, Sci. Rep. **4** (2014).
[31] P. London, P. Balasubramanian, B. Naydenov, L. P. McGuinness, and F. Jelezko, Phys. Rev. A **90**, 012302 (2014).
[32] G. D. Fuchs, V. V. Dobrovitski, D. M. Toyli, F. J. Heremans, and D. D. Awschalom, Science **326**, 1520 (2009).
[33] J. Yoneda, T. Otsuka, T. Nakajima, T. Takakura, T. Obata, M. Pioro-Ladrière, H. Lu, C. Palmstrøm, A. C. Gossard, and S. Tarucha, arXiv:1411.6738 (2014).
[34] N. L. Schryer and L. R. Walker, J. App. Phys. **45**, 5406 (1974).
[35] G. Balasubramanian, P. Neumann, D. Twitchen, M. Markham, R. Kolesov, N. Mizuochi, J. Isoya, J. Achard, J. Beck, J. Tissler, V. Jacques, P. R. Hemmer, F. Jelezko, and J. Wrachtrup, Nat. Mater **8**, 383 (2009).
[36] J.-P. Tetienne, L. Rondin, P. Spinicelli, M. Chipaux, T. Debuisschert, J.-F. Roch, and V. Jacques, New J. of Phys. **14**, 103033 (2012).
[37] V. M. Acosta, E. Bauch, M. P. Ledbetter, C. Santori, K.-M. C. Fu, P. E. Barclay, R. G. Beausoleil, H. Linget, J. F. Roch, F. Treussart, S. Chemerisov, W. Gawlik, and D. Budker, Phys. Rev. B **80**, 115202 (2009).
[38] E. Schäfer-Nolte, L. Schlipf, M. Ternes, F. Reinhard, K. Kern, and J. Wrachtrup, ArXiv e-prints (2014), arXiv:1406.0362.
[39] E. Schäfer-Nolte, L. Schlipf, M. Ternes, F. Reinhard, K. Kern, and J. Wrachtrup, Phys. Rev. Lett. **113**, 217204 (2014).
[40] D. O. Smith, J. App. Phys. **29**, 264 (1958).
[41] J. Lotze, H. Huebl, R. Gross, and S. T. B. Goennenwein, Phys. Rev. B **90**, 174419 (2014).
[42] M. Julliere, Phys. Lett. A **54**, 225 (1975).
[43] K.-J. Lee, A. Deac, O. Redon, J.-P. Nozieres, and B. Dieny, Nat. Mater **3**, 877 (2004).
[44] J. Teissier, A. Barfuss, P. Appel, E. Neu, and P. Maletinsky, Phys. Rev. Lett. **113**, 020503 (2014).
[45] A. Aharoni, *Introduction to the Theory of Ferromagnetism*, 2nd ed. (Oxford University Press, Oxford ; New York, 2001).
[46] V. N. Samofalov, D. P. Belozorov, and A. G. Ravlik, Physics-Uspekhi **56**, 269 (2013).
[47] The code is available at http://math.nist.gov/oommf.
[48] G. D. Fuchs, G. Burkard, P. V. Klimov, and D. D. Awschalom, Nat. Phys **7**, 789 (2011).